Transcription factor JDP2 activates PDE4B to participate in hypoxia/reoxygenation-induced H9c2 cell injury

SUIPENG LI, YONG CHEN, YINFENG JIA, TINGTING XUE, XUQING HOU and ZHANGYIN ZHAO

Department of Cardiology, The Second People's Hospital of Yueqing, Yueqing, Zhejiang 325600, P.R. China

Received June 30, 2021; Accepted September 21, 2021

DOI: 10.3892/etm.2022.11270

Abstract. Myocardial ischemia/reperfusion (I/R) injury is a clinical challenge in the treatment of acute myocardial infarction (AMI). Phosphodiesterase 4B (PDE4B) expression is upregulated in AMI tissues. Thus, the present study aimed to investigate the role of PDE4B in myocardial I/R injury. H9c2 cardiomyocytes were subjected to hypoxia/reoxygenation (H/R) to establish an *in vitro* myocardial I/R model. PDE4B expression was detected via reverse transcription-quantitative PCR (RT-qPCR) and western blotting before and after transfection with PDE4B interference plasmids in H/R-stimulated H9c2 cells. Cell viability and cytotoxicity were assessed using the Cell Counting Kit-8 and lactate dehydrogenase assays, respectively. Furthermore, oxidative stress was assessed using malondialdehyde, superoxide dismutase and glutathione/glutathione oxidized ratio detection kits. Cell apoptosis was detected via a TUNEL assay and western blotting. c-Jun dimerization protein 2 (JDP2) expression was also detected via RT-qPCR and western blotting. The dual luciferase reporter and chromatin immunoprecipitation assays were performed to verify the interaction between JDP2 and PDE4B. Following co-transfection with PDE4B interference plasmid and JDP2 overexpression plasmid, cell viability, cytotoxicity, oxidative stress and cell apoptosis were assessed. The results demonstrated that PDE4B knockdown reversed H/R-induced loss of viability and cytotoxicity of H9c2 cells. H/R-induced oxidative stress and cardiomyocyte apoptosis were also alleviated by PDE4B knockdown. In addition, the transcription factor JDP2 was expressed at high levels in H/R-stimulated H9c2 cells, and JDP2 overexpression upregulated PDE4B expression. Notably, JDP2 overexpression partly reversed the ameliorative effect of PDE4B knockdown on H/R-induced H9c2 injury. Taken together, the results of the present study suggested that JDP2-activated PDE4B contributed to H/R-induced H9c2 cell injury.

Correspondence to: Dr Suipeng Li, Department of Cardiology, The Second People's Hospital of Yueqing, 26 Feihong North Road, Hongqiao, Yueqing, Zhejiang 325600, P.R. China
E-mail: lisuipengyx@163.com

Key words: acute myocardial infarction, hypoxia/reoxygenation, myocardial ischemia/reperfusion injury, c-Jun dimerization protein 2, phosphodiesterase 4B

Introduction

Acute myocardial infarction (AMI) is characterized by myocardial necrosis caused by acute and persistent ischemia and hypoxia of cardiac cells (1). Clinically, AMI presents as sharp and persistent substernal pain that cannot be fully relieved by resting or nitrate medications, and is accompanied by elevated levels of serum myocardial enzymes, including creatine kinase and lactate dehydrogenase (LDH), as well as abnormal progression on an electrocardiogram (2-4). AMI can occur at the same time as arrhythmias, shock or heart failure, and is often life threatening. This disease is most common in North American and European countries, where ~1.5 million new cases of AMI are reported in the United States annually (5,6). In China, the incidence of AMI has continued to increase in the last decade, with ≥500,000 new cases annually and ~2 million patients currently diagnosed (7). Myocardial ischemia/reperfusion (I/R) injury is often the result of different types of coronary artery disease, including myocardial infarction, ischemic cardiomyopathy and sudden coronary death (8). Reperfusion is a standard therapy for acute cases of coronary artery diseases, including MI, and is also an inevitable inducer of I/R injury of coronary microvessels and myocardium (9-11).

Phosphodiesterase 4B (PDE4B) is one of the 11 members of the PDE enzyme family that are known for their exclusive ability to decompose cyclic nucleotides, and it can regulate several biological processes (12). A recent microarray study identified PDE4B as a metabolism-related gene that was strongly associated with the onset and recurrence of AMI (13). Previous studies have reported that activation of PDE4B induced cognitive impairment and neuronal apoptosis, and aggravated neuroinflammation and oxidative stress in the central nervous system (14,15).

Jun dimerization protein 2 (JDP2) is a bZip-type transcription factor that belongs to the activator protein-1 (AP-1) family (16). JDP2 upregulation in mice has been reported to have a direct association with impaired cardiac function manifested as cardiomyocyte apoptosis, cardiac hypertrophy, fibrosis and inflammation (17).

Therefore, the present study aimed to investigate how PDE4B expression affected myocardial hypoxia/reoxygenation (H/R) injury, and to determine the function of JDP2 in the process.

Materials and methods

Bioinformatics tools. JASPAR database (jaspar.genereg.net) which is a regularly maintained open-access database storing manually curated transcription factors (TF) binding profiles as position frequency matrices (PFMs) was applied to predict the interaction between the transcription factor JDP2 and PDE4B promoter.

Cell culture and treatment. H9c2 rat embryo heart-derived cardiomyocytes (American Type Culture Collection) were cultured in low-glucose DMEM supplemented with 10% FBS (Gibco, Thermo Fisher Scientific, Inc.) in a 5% CO_2 incubator at 37˚C. To create a hypoxic condition, H9c2 cells were cultured at 37˚C for 6 h in serum-free and glucose-free DMEM in a tri-gas incubator with 94% N_2, 5% CO_2 and 1% O_2. Subsequently, cells were re-oxygenated for 2 h in DMEM supplemented with 10% FBS in 95% air and 5% CO_2 at 37˚C, as previously described (18). Cells incubated in a humidified atmosphere of 5% CO_2 incubator at 37˚C for 20 h were used as a control throughout the experiments.

Cell transfection. Short hairpin (sh)RNA plasmids specific for PDE4B which were ligated into the plasmid of U6/GFP/Neo [sh-PDE4B-1 forward, 5'-CCGGTACTCCTTCTCTGTGAAATTTCTCGAGAAATTTCACAGAGAAGGAGTATTTTTG-3' and reverse, 5'-AATTCAAAAATACTCCTTCTCTGTGAAATTTCTCGAGAAATTTCACAGAGAAGGAGTA-3'; sh-PDE4B-2 forward, 5'-CCGGTCCATCTACAGTCTGAGATTACTCGAGTAATCTCAGACTGTAGATGGATTTTTG-3' and reverse, 5'-AATTCAAAAATCCATCTACAGTCTGAGATTACTCGAGTAATCTCAGACTGTAGATGGA-3', shRNA with empty vectors which was regarded as negative control (NC), pcDNA3.1(+) JDP2 overexpression vector (Oe-JDP2) and Oe-NC were purchased from Shanghai GenePharma Co., Ltd. H9c2 cells ($4x10^5$ cells/well) were transfected with 50 nM sh-PDE4B-1/2, sh-NC, Oe-JDP2 or Oe-NC using Lipofectamine® 2000 (Invitrogen; Thermo Fisher Scientific, Inc.) according to the manufacturer's protocol. After incubation at 37˚C for 48 h, cells were harvested for subsequent experiments.

Reverse transcription-quantitative PCR (RT-qPCR). Total RNA was extracted from H9c2 cells using the RNAeasy™ Viral RNA Isolation kit with Spin Column (Beyotime Institute of Biotechnology). Total RNA was reverse transcribed into cDNA using the Revert Aid™ cDNA Synthesis kit (Takara Biotechnology co., Ltd.) according to the manufacturer's protocol. Subsequently, qPCR was performed using BeyoFast™ Probe qPCR mix (Beyotime Institute of Biotechnology). The thermocycling conditions were as follows: Pre-denaturation at 95˚C for 30 sec, followed by denaturation at 95˚C for 10 sec and annealing at 55˚C for 30 sec for 40 cycles. The following primers were used for qPCR: PDE4B forward, 5'-ACGGTGGCTCATACATGCT-3' and reverse, 5'-GTACCAGTCCCGACGAAGAG-3'; JDP2 forward, 5'-CCCAGGGACCTCGAGCTTT-3' and reverse, 5'-GGTCTTCAGCTCTGCGTTCA-3'; and GADPH forward, 5'-GAATGGGCAGCCGTTAGGAA-3' and reverse, 5'-AAAAGCATCACCCGGAGGAG-3'. Relative expression levels were calculated using the $2^{-\Delta\Delta Cq}$ method (19) and normalized to the internal reference gene GAPDH.

Western blotting. Total protein was extracted from H9c2 cells using RIPA lysis buffer (Shanghai Yeasen Biotechnology Co., Ltd.) and quantified using a BCA kit (Shanghai Enzyme-linked Biotechnology Co., Ltd.). Proteins (20 μg per lane) were separated via 10% SDS-PAGE (Beyotime Institute of Biotechnology) and transferred onto PVDF membranes. The membranes were incubated at 4˚C overnight with primary antibodies targeted against: PDE4B (1:1,000; cat. no. ab14628; Abcam), Bcl-2 (1:1,000; cat. no. ab196495; Abcam), Bax (1:1,000; cat. no. ab32503; Abcam), cleaved-caspase3 (1:1,000; cat. no. 9661; Cell Signaling Technology, Inc.), cleaved-caspase9 (1:1,000; cat. no. 10380-1-AP; ProteinTech Group, Inc.), JDP2 (1:1,000; cat. no. orb336272; Biorbyt Ltd.) and GAPDH (1:10,000; cat. no. ab181602; Abcam). Following the primary incubation, membranes were incubated with a HRP-labeled Goat Anti-Rabbit IgG (H+L) secondary antibody (1:1,000; cat. no. A0208; Beyotime Institute of Biotechnology) at 37˚C for 2 h. Protein bands were visualized using ECL reagents (PerkinElmer, Inc.) and analyzed by Image J software (version 1.48v; National Institutes of Health). GAPDH was used as the loading control.

Cell viability and cytotoxicity. The Cell Counting Kit-8 (CCK-8; Beijing Solarbio Science & Technology Co., Ltd.) assay was performed was to assess cell viability. Briefly, H9c2 cells ($2x10^3$ cells/100 μl/well) were incubated with 10 μl/well CCK-8 solution in a 96-well plate for 2 h. Subsequently, optical density was measured at a wavelength of 450 nm using a microplate reader (Bio-Rad Laboratories, Inc.).

The LDH Cytotoxicity Assay Kit (Beyotime Institute of Biotechnology) was used to detect H/R-induced cytotoxicity according to the manufacturer's instructions. LDH activity was measured at a wavelength of 490 nm using a microplate reader (Bio-Rad Laboratories, Inc.).

Detection of oxidative stress levels. The levels of malondialdehyde (MDA) and superoxide dismutase (SOD) in H9c2 cells were detected using MDA (A003-1-2) and SOD (A001-3-2) assay kits (both Nanjing Jiancheng Bioengineering Institute), respectively. The glutathione (GSH) to glutathione oxidized (GSSG) ratio was measured using the GSH/GSSG Ratio Assay kit (cat. no. KA6046; Abnova). Briefly, the cell precipitate was collected via centrifugation at 1,600 x g for 10 min at 4˚C and freeze-thawed twice with liquid nitrogen and 37˚C water baths prior to centrifugation at 1,000 x g for 10 min at room temperature. Subsequently, working solution and NADPH solution from the kits were prepared and added successively into the supernatant. Following incubation, the absorbance at 412 nm was determined using a microplate reader (BioTek instruments, inc.).

Measurement of apoptotic rate and apoptosis-related proteins. H9c2 cell apoptosis was detected using the TUNEL Apoptosis Assay kit (Beyotime Institute of Biotechnology). After washing with PBS, cells were fixed with 4% paraformaldehyde at 4˚C for 10 min, permeabilized with 0.3% PBS in Triton X-100 at room temperature for 30 min and then

incubated with 0.3% H_2O_2 in PBS on ice for 2 min prior to biotin labeling. Cells were incubated with TUNEL detection solution at 37˚C for 60 min in the dark and stained with 10 μg/ml DAPI (Shanghai Haoyang Bio Technology Co., Ltd.) at 37˚C for 2-3 min. In total, three fields of view were selected at random and the images were captured using a fluorescence microscope (magnification, x200; Olympus Corporation). Apoptosis-related protein expression levels were detected via western blotting according to the aforementioned protocol.

Verification of interaction between JDP2 and PDE4B. For the dual luciferase reporter assay, H9c2 cells ($5x10^5$ cells/well) were seeded ($1x10^4$ cells/well) into 96-well plates. Subsequently, H9c2 cells were co-transfected with PDE4B-WT and PDE4B-MUT, Oe-JDP2 or Oe-NC (0.5 μg) and *Renilla* luciferase reporter vector (Promega Corporation) using Lipofectamine® 2000 (Invitrogen; Thermo Fisher Scientific, Inc.) for 48 h at 37˚C. At 48 h post-transfection, firefly luciferase activities was measured using a Dual Luciferase Reporter Assay system (Promega Corporation) and normalized to *Renilla* luciferase activities.

For the chromatin immunoprecipitation (ChIP) assay, ultrasound-treated samples were centrifuged at 12,000-14,000 x g for 5 min at 4˚C. A total of 300 μl SDS lysis buffer (Active Motif, Inc.) was then used to lyse the cells, which were subsequently sonicated at 150 Hz and sheared with four sets of 10 sec pulses on wet ice using a high intensity ultrasonic processor. ChIP Dilution Buffer containing 1 mM PMSF was prepared using the ChIP Assay kit (Beyotime Institute of Biotechnology) and added to part of the samples to serve as the input. A total of 40 μl protein A/G agarose beads (Santa Cruz Biotechnology, Inc.) was added to the rest of the samples. Following centrifugation at 16,000 x g for 10 min at 4˚C, supernatant (100 μl) was incubated with 5 μg anti-IgG (cat. no. sc-2025; Santa Cruz Biotechnology, Inc.) or anti-JDP2 (cat. no. sc-517133; Santa Cruz Biotechnology, Inc.) primary antibodies and protein A/G agarose at 4˚C overnight. The precipitated chromatin was purified by phenol/chloroform/isoamyl extraction and analyzed via RT-qPCR according to the aforementioned protocol.

Statistical analysis. Statistical analyses were performed using GraphPad Prism (version 8; GraphPad Software, Inc.). All experiments were performed in triplicate. Data are presented as the mean ± SD from at least three independent experiments. Comparisons between two groups were analyzed using an unpaired Student's t-test, whereas comparisons among multiple groups were analyzed using one-way ANOVA followed by Tukey's post hoc test. $P<0.05$ was considered to indicate a statistically significant difference.

Results

Effect of PDE4B knockdown on H9c2 cell viability and cytotoxicity following H/R. Firstly, H9c2 cells were transfected with sh-PDE4B-1/2 or sh-NC, and then PDE4B expression was detected via RT-qPCR and western blotting (Fig. 1A and B). sh-PDE4B-1 and sh-PDE4B-2 significantly decreased PDE4B expression levels compared with sh-NC. Moreover, PDE4B was expressed at significantly higher levels in H9c2 cells exposed to H/R compared with the control group (Fig. 1C and D). In addition, transfection with sh-PDE4B-1/2 significantly decreased the expression of PDE4B under H/R conditions, with sh-PDE4B-1 displaying a higher knockdown effect compared with sh-PDE4B-2 (Fig. 1C and D). Thus, sh-PDE4B-1 was selected for use in subsequent experiments. Compared with the control group, cells exposed to H/R displayed a significant decline in viability, whereas PDE4B interference significantly increased cell viability under H/R conditions (Fig. 1E). Cytotoxicity detection in H9c2 cells demonstrated that PDE4B knockdown significantly decreased H/R-induced upregulated LDH levels (Fig. 1F). Taken together, these results suggested that PDE4B knockdown prevented decreases in cell viability and alleviated the cytotoxicity of H/R-stimulated H9c2 cells.

Effect of PDE4B knockdown on H/R-induced oxidative stress and apoptosis in H9c2 cells. The present study assessed the degrees of oxidative stress and apoptosis of H9c2 cells following H/R, before and after transfection with sh-PDE4B. The results demonstrated that the concentration of MDA was significantly higher (Fig. 2A), whereas the concentration of SOD and the GSH/GSSG ratio were significantly lower (Fig. 2B and C) in cells exposed to H/R compared with those in the control group. However, PDE4B knockdown significantly decreased the concentration of MDA, and significantly elevated the concentration of SOD and the ratio of GSH to GSSG under H/R conditions. In addition, the number of $TUNEL^+$ cells was significantly increased in the H/R group compared with the control group, which was significantly reversed following PDE4B knockdown (Fig. 3A). Consistently, in H/R-stimulated H9c2 cells, anti-apoptotic Bcl-2 expression was significantly decreased, whereas proapoptotic Bax expression was significantly increased, and the expression levels of cleaved-caspase3 and cleaved-caspase9 were significantly increased compared with those in the control group. Notably, these effects were significantly reversed following PDE4B knockdown (Fig. 3B). Collectively, these results suggested that PDE4B knockdown ameliorated H/R-induced oxidative stress and apoptosis in H9c2 cells.

Binding interaction between PDE4B and transcription factor JDP2. RT-qPCR and western blotting confirmed that JDP2 expression was upregulated in H9c2 cells following H/R (Fig. 4A and B). JASPAR was used to predict the binding sites between JDP2 and PDE4B (Fig. 4C). This interaction was confirmed by performing dual luciferase reporter and ChIP assays, which demonstrated significantly upregulated luciferase activities in cells co-transfected with PDE4B-wild-type (WT) and Oe-JDP2 compared with those co-transfected with PDE4B-WT and Oe-NC. No apparent changes were observed in the luciferase activity of PDE4B-MUT after co-transfection of Oe-NC or Oe-JDP2 (Fig. 4D). Compared with cells treated with IgG, significantly increased PDE4B expression was observed in cells treated with anti-JDP2 (Fig. 4E). The RT-qPCR results confirmed the successful transfection of Oe-JDP2 in H9c2 cells (Fig. 4F). mRNA level of PDE4B was also enhanced after transfection of Oe-JDP2 (Fig. 4G). Additionally, the results demonstrated that JDP2 overexpression significantly increased PDE4B expression in H9c2 cells exposed to H/R

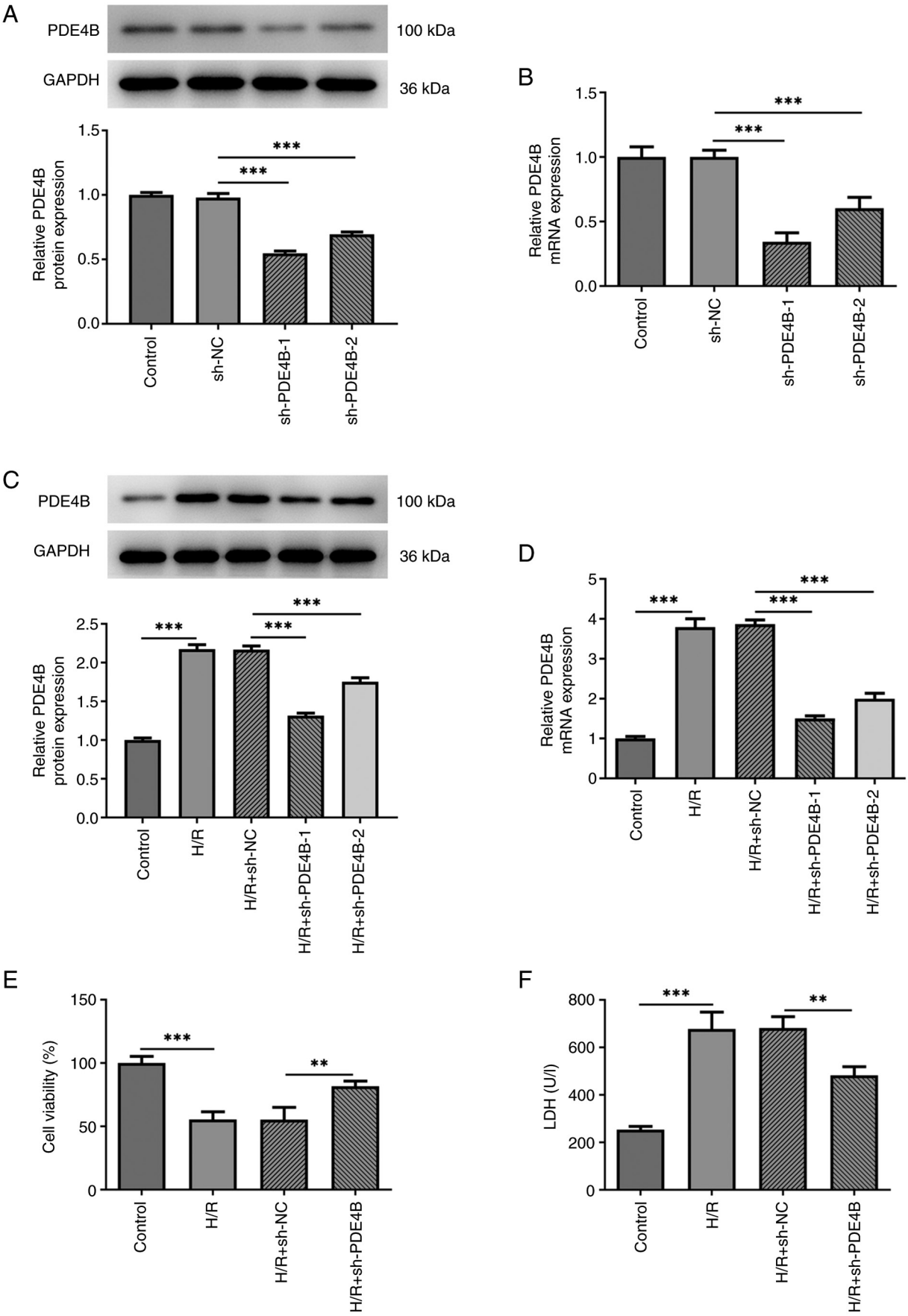

Figure 1. PDE4B knockdown increases H9c2 cell viability and decreases cytotoxicity following H/R injury. (A) Western blotting and (B) RT-qPCR were performed to detect the transfection efficiency of PDE4B knockdown. (C) Western blotting and (D) RT-qPCR were performed to detect PDE4B expression in H/R-stimulated H9c2 cells following PDE4B knockdown. (E) Cell viability and (F) cytotoxicity in H/R-stimulated H9c2 cells following PDE4B knockdown were assessed using Cell Counting Kit-8 and lactate dehydrogenase assays, respectively. **P<0.01 and ***P<0.001. PDE4B, phosphodiesterase 4B; H/R, hypoxia/reoxygenation; sh, short hairpin RNA; NC, negative control; LDH, lactate dehydrogenase; RT-qPCR, reverse transcription-quantitative PCR.

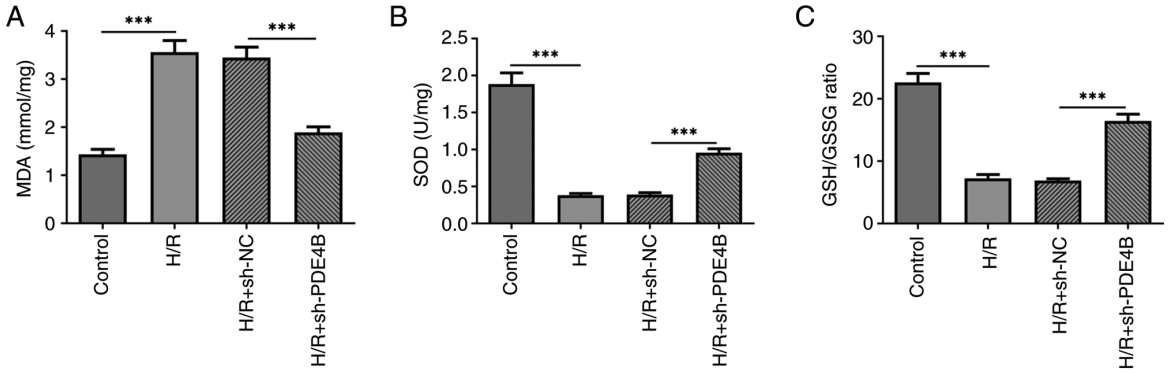

Figure 2. PDE4B knockdown ameliorates H/R-induced oxidative stress in H9c2 cells. Commercial kits were used to detect (A) MDA concentration, (B) SOD concentration and (C) the ratio of GSH to GSSG in H/R-stimulated H9c2 cells following PDE4B knockdown. ***P<0.001. PDE4B, phosphodiesterase 4B; H/R, hypoxia/reoxygenation; MDA, malondialdehyde; SOD, superoxide dismutase; GSH, glutathione; GSSG, glutathione oxidized; sh, short hairpin RNA; NC, negative control.

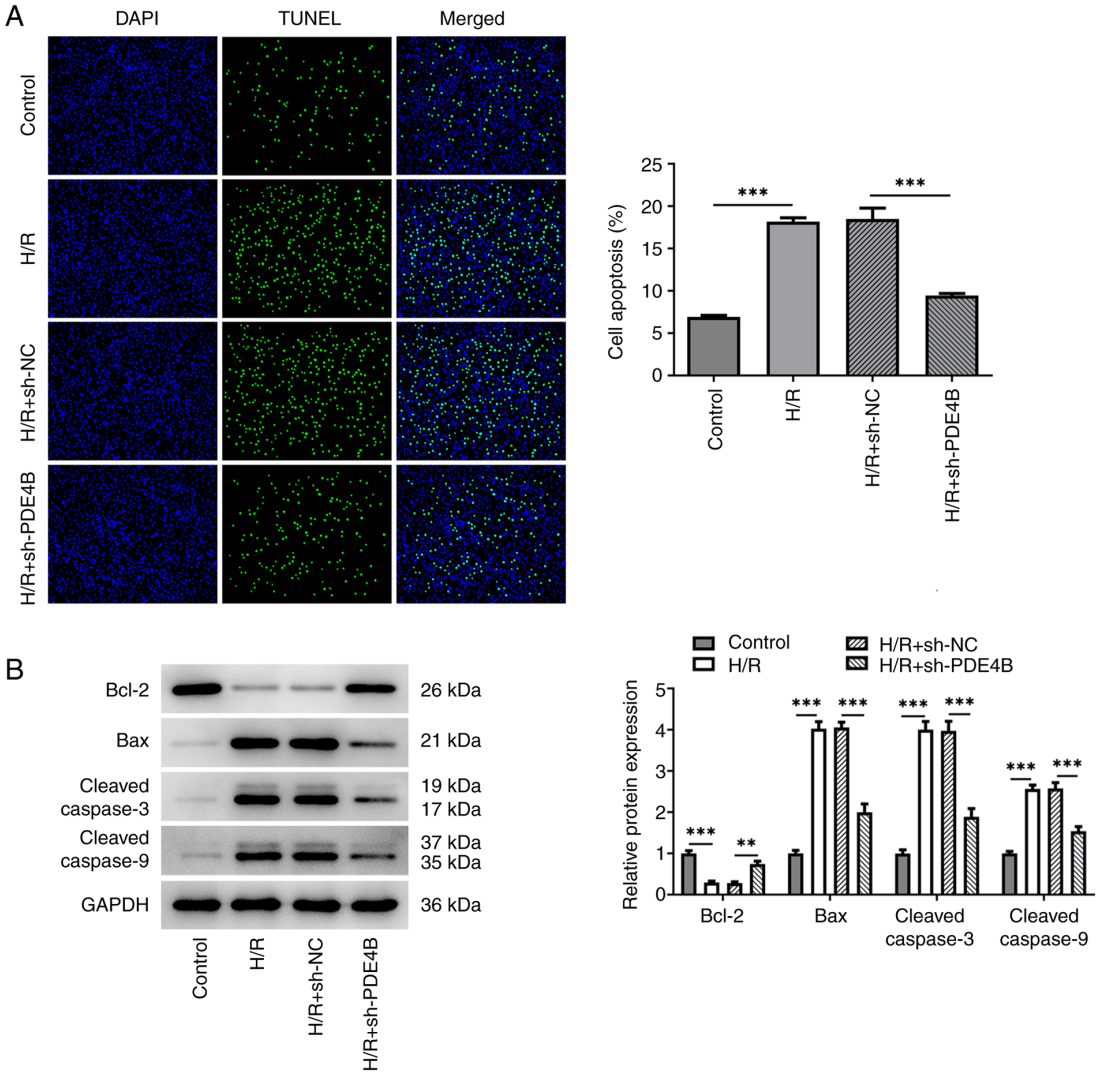

Figure 3. PDE4B knockdown suppresses H/R-induced H9c2 cell apoptosis. (A) Cell apoptosis was determined by assessing the number of TUNEL+ cells (green fluorescence). (B) Western blotting was performed to detect the expression levels of apoptosis-related proteins. **P<0.01 and ***P<0.001. PDE4B, phosphodiesterase 4B; H/R, hypoxia/reoxygenation; sh, short hairpin RNA; NC, negative control.

(Fig. 4H). Taken together, these results suggested that the transcription factor JDP2 activated PDE4B in H9c2 cells exposed to H/R.

Role of JDP2 in PDE4B knockdown-mediated alleviation of H9c2 cell injury following H/R. The present study investigated how the interaction between JDP2 and PDE4B

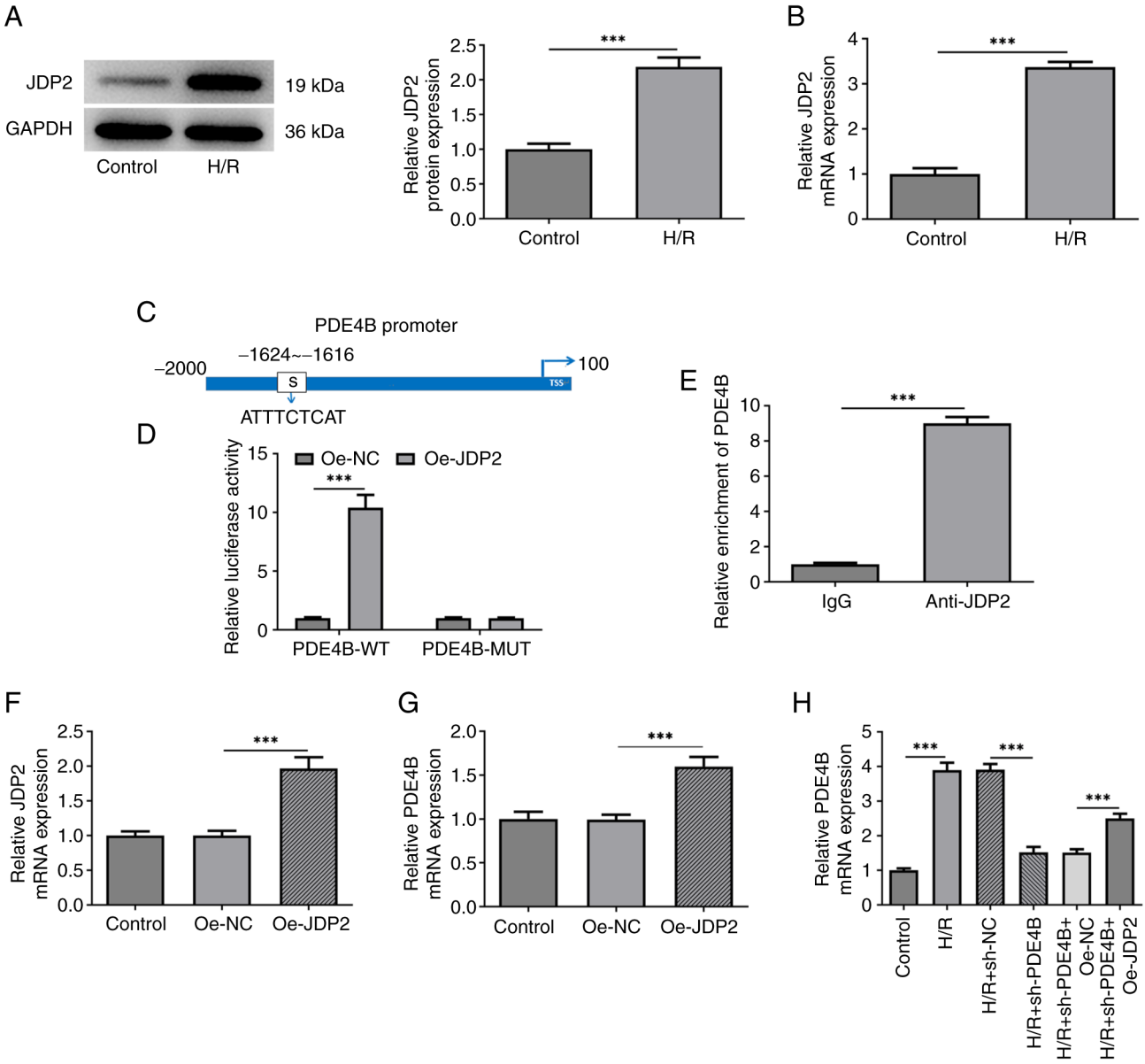

Figure 4. JDP2 expression is upregulated in H/R-stimulated H9c2 cells, which activates PDE4B expression. (A) Western blotting and (B) RT-qPCR were performed to detect JDP2 expression in H/R-stimulated H9c2 cells. (C) JASPAR database was used to predict the binding sites between JDP2 and PDE4B promoter regions. (D) Dual luciferase reporter assays were performed to detect relative luciferase activities in cells co-transfected with PDE4B-WT or MUT and Oe-NC or Oe-JDP2. (E) Chromatin immunoprecipitation assays were performed to detect PDE4B enrichment in IgG and anti-JDP2 groups. (F) RT-qPCR was performed to assess the transfection efficiency of Oe-JDP2 in H9c2 cells. (G) RT-qPCR was performed to detect PDE4B mRNA expression levels after JDP2 overexpression in H9c2 cells. (H) RT-qPCR was performed to detect PDE4B mRNA expression in H/R-stimulated H9c2 cells following transfection with sh-PDE4B or co-transfection with Oe-JDP2. ***P<0.001. JDP2, c-Jun dimerization protein 2; H/R, hypoxia/reoxygenation; PDE4B, phosphodiesterase 4B; RT-qPCR, reverse transcription-quantitative PCR; WT, wild-type; MUT, mutant; Oe, overexpression; NC, negative control; sh, short hairpin RNA.

affected H/R-induced H9c2 cell injury. Analysis of cell viability and cytotoxicity under H/R conditions demonstrated a significant decrease in H9c2 cell viability (Fig. 5A) and a significant increase in the level of LDH (Fig. 5B) following co-transfection with sh-PDE4B and Oe-JDP2 compared with that observed in sh-PDE4B + Oe-NC group. Therefore, the results indicated that JDP2 overexpression reversed the effect of PDE4B knockdown on H/R-induced H9c2 cell injury.

Role of JDP2 in PDE4B interference-alleviated oxidative stress and apoptosis of H9c2 cells following H/R. The results demonstrated significantly increased MDA concentration (Fig. 5C), and significantly decreased SOD concentration (Fig. 5D) and GSH/GSSG ratio (Fig. 5E) in H/R-stimulated H9c2 cells co-transfected with sh-PDE4B and Oe-JDP2 compared with those co-transfected with sh-PDE4B and Oe-NC. Notably, JDP overexpression significantly increased the number of TUNEL$^+$ cells (Fig. 6A), decreased Bcl-2 expression, increased Bax expression, and increased the expression levels of cleaved-caspase3 and cleaved-caspase9 following H/R in PDE4B-knockdown H9c2 cells (Fig. 6B). Collectively, these results suggested that JDP2 overexpression reversed the ameliorative effect of PDE4B knockdown on H/R-induced oxidative stress and apoptosis in H9c2 cells.

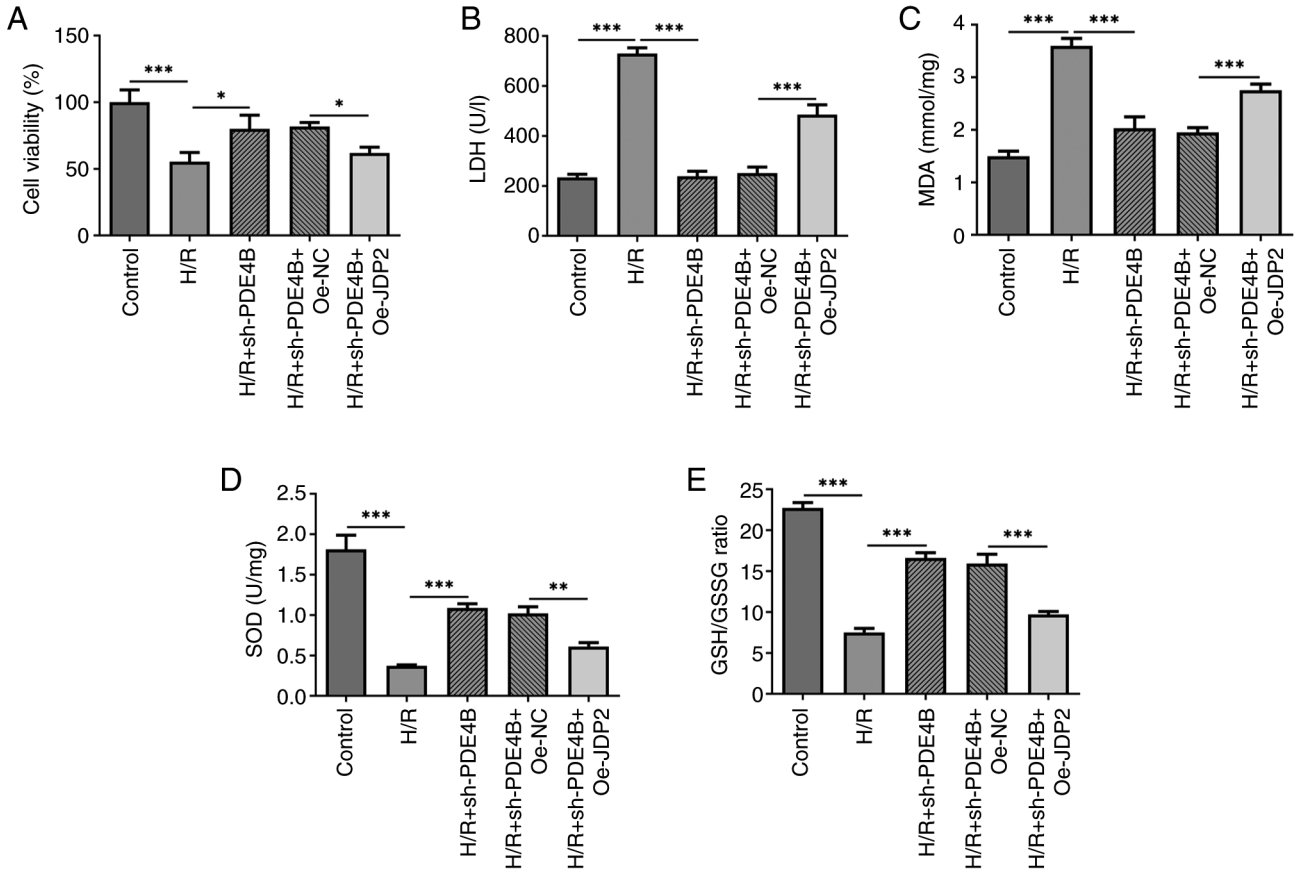

Figure 5. JDP2 overexpression partly reverses the effects of PDE4B knockdown on cell viability, cytotoxicity and oxidative stress in H/R-stimulated H9c2 cells. Analysis of (A) cell viability, (B) cytotoxicity, (C) MDA concentration, (D) SOD concentration and (E) GSH/GSSG ratio in H/R-stimulated H9c2 cells following transfection with sh-PDE4B or co-transfection with Oe-JDP2. *P<0.05, **P<0.01 and ***P<0.001. JDP2, c-Jun dimerization protein 2; PDE4B, phosphodiesterase 4B; H/R, hypoxia/reoxygenation; MDA, malondialdehyde; SOD, superoxide dismutase; GSH, glutathione; GSSG, glutathione oxidized; sh, short hairpin RNA; Oe, overexpression; NC, negative control; LDH, lactate dehydrogenase.

Discussion

AMI is a serious consequence of atherosclerotic cardiovascular disease and coronary artery disease. Rapid development of cardiac interventional therapy and bypass surgery has improved the treatment of coronary heart disease (20). However, several issues associated with AMI treatment remain, particularly cardiomyocyte necrosis or apoptosis from prolonged myocardial ischemia (21,22). Myocardial I/R injury is the primary pathological manifestation of coronary artery disease, which continues to increase the global morbidity and mortality of AMI despite therapeutic intervention (23). Cytotoxic oxygen species production, inflammatory response, oxidative stress, and interplay between apoptosis and autophagy are critical participants in I/R-induced cardiomyocyte injury (24-26).

Previous studies have reported the roles of certain genes in the process of AMI (27-29). In the present study, a high expression level of PDE4B expression was observed in H9c2 cardiomyocytes exposed to H/R, indicating the involvement of PDE4B in H/R-induced AMI. Aberrantly high PDE4B expression has been identified as a contributing factor in the pathogenesis of several diseases, including colorectal cancer, neurological conditions and injury, allergy and heart failure (30-33). In the setting of oxygen-glucose deprivation-induced HT22 mouse hippocampal neuronal cell injury, PDE4B overexpression promotes endoplasmic reticulum stress and the release of reactive oxygen species (34). Furthermore, PDE4B knockdown in primary microglia increases LC-3II expression and decreases inflammasome activity (35). The results of the present study demonstrated that PDE4B knockdown increased H9c2 viability and decreased cytotoxicity under H/R conditions. According to a study on acute lung injury, PDE4B knockout could effectively inhibit lipopolysaccharide (LPS)-induced activation of the NF-κB-related inflammatory response and generation of reactive oxygen species in multiple pulmonary cell lines, including epithelial cells (A549), microvascular endothelial cells (pulmonary microvascular endothelial cells) and vascular smooth muscle cells (36). PDE4B has also been reported to be upregulated in patients with acute kidney injury, whereas treatment with rutaecarpine derivative compound-6c exerts an anti-oxidative effect by downregulating PDE4B to protect kidney tubular epithelial cells against oxidative stress and programmed cell death (37). The results of the present study demonstrated that PDE4B knockdown alleviated H/R-induced oxidative stress and apoptosis in H9c2 cardiomyocytes, which was consistent with previous findings.

In the present study, the JASPAR database was used to predict the binding sites between PDE4B promoter and JDP2, a transcription factor that is differentially expressed

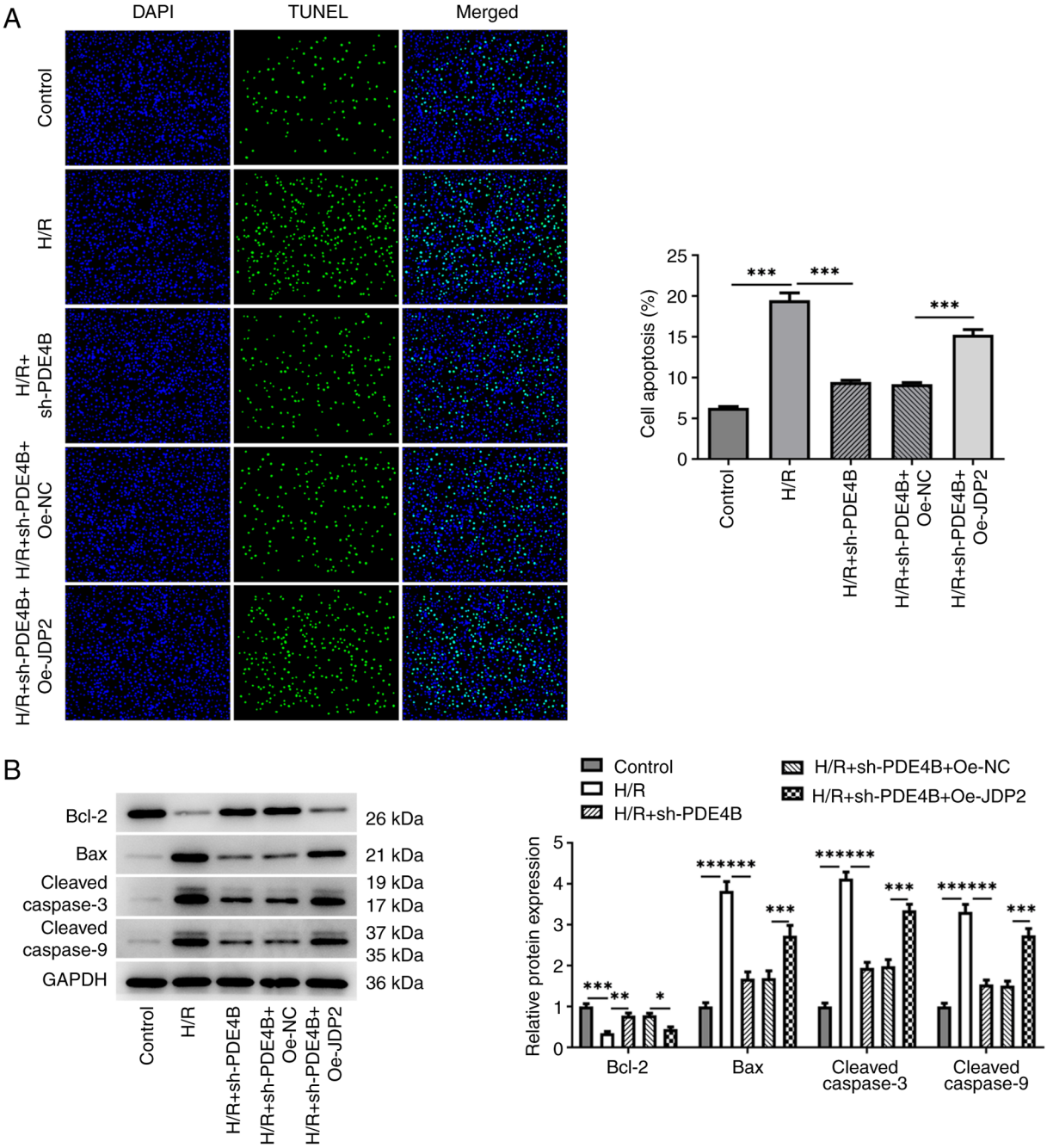

Figure 6. JDP2 overexpression partly reverses effect of PDE4B knockdown on H/R-induced cell apoptosis. (A) Apoptotic H9c2 cells and (B) the expression of apoptosis-related proteins in H/R-stimulated H9c2 cells following transfection with sh-PDE4B or co-transfection with Oe-JDP2. *P<0.05, **P<0.01 and ***P<0.001. JDP2, c-Jun dimerization protein 2; PDE4B, phosphodiesterase 4B; H/R, hypoxia/reoxygenation; sh, short hairpin RNA; Oe, overexpression; NC, negative control.

in patients with MI (38). In view of the critical regulatory role of JDP2 in impaired cardiac function (17), the present study also confirmed that JDP2 was upregulated in H9c2 cells exposed to H/R, and verified the interaction between JDP2 and the PDE4B promoter region. In addition, JDP2 expression is activated by hypoxia in a murine model of MI and is regulated by testis-specific transcript, Y-linked 15-targeted microRNA-455-5p to prevent cardiomyocyte apoptosis and rescue cell migration and invasion (39). In mice with traumatic brain injury, LPS stimulates the expression of JDP2, and JDP2 overexpression aggravates LPS-induced inflammation and apoptosis of mouse astrocytes (40). Consistent with these findings, the results of the present study demonstrated that JDP2 overexpression attenuated the ameliorative effect of PDE4B knockdown on cell viability, cytotoxicity, oxidative stress and apoptosis in H/R-stimulated H9c2 cardiomyocytes.

In conclusion, the results of the present study demonstrated that the transcription factor JDP2 activated PDE4B expression to participate in H/R-induced oxidative and apoptotic injuries of H9c2 cardiomyocytes, partially explaining the pathogenic mechanism underlying myocardial I/R injury. Taken together, the results of the present study suggested that PDE4B and JDP2 may serve as promising biomarkers and therapeutic targets in

AMI diagnosis and treatment. However, further *in vivo* studies are required to confirm the results of the present study.

Acknowledgements

Not applicable.

Funding

No funding was received.

Availability of data and materials

The datasets used and/or analyzed during the current study are available from the corresponding author on reasonable request.

Authors' contributions

SL and ZZ were responsible for the conception of the study and the drafting of the manuscript. SL, YC, YJ, TX and XH assisted in obtaining experimental data and analyzed the data. ZZ revised the manuscript. SL and ZZ confirm the authenticity of all the raw data. All authors have read and approved the final manuscript.

Ethics approval and consent to participate

Not applicable.

Patient consent for publication

Not applicable.

Competing interests

The authors declare that they have no competing interests.

References

1. Pollard TJ: The acute myocardial infarction. Prim Care 27: 631-649;vi, 2000.
2. Beltrame JF: Nitrate therapy in acute myocardial infarction: Potion or poison? Cardiovasc Drugs Ther 22: 165-168, 2008.
3. Jensen AE, Reikvam A and Asberg A: Diagnostic efficiency of lactate dehydrogenase isoenzymes in serum after acute myocardial infarction. Scand J Clin Lab Invest 50: 285-289, 1990.
4. Hurst JW: Thoughts about the abnormalities in the electrocardiogram of patients with acute myocardial infarction with emphasis on a more accurate method of interpreting ST-segment displacement: Part I. Clin Cardiol 30: 381-390, 2007.
5. Sattar Y and Alraies MC: Ventricular aneurysm. In: StatPearls. StatPearls Publishing, Treasure Island, FL, 2021.
6. Lindower P, Embrey R and Vandenberg B: Echocardiographic diagnosis of mechanical complications in acute myocardial infarction. Clin Intensive Care 4: 276-283, 1993.
7. Li J, Li X, Wang Q, Hu S, Wang Y, Masoudi FA, Spertus JA, Krumholz HM and Jiang L; China PEACE Collaborative Group: ST-segment elevation myocardial infarction in China from 2001 to 2011 (the China PEACE-retrospective acute myocardial infarction study): A retrospective analysis of hospital data. Lancet 385: 441-451, 2015.
8. Neri M, Riezzo I, Pascale N, Pomara C and Turillazzi E: Ischemia/reperfusion injury following acute myocardial infarction: A critical issue for clinicians and forensic pathologists. Mediators Inflamm 2017: 7018393, 2017.
9. Bagai A, Dangas GD, Stone GW and Granger CB: Reperfusion strategies in acute coronary syndromes. Circ Res 114: 1918-1928, 2014.
10. Borer JS and Lewis BS: Therapeutic coronary reperfusion and reperfusion injury: An introduction. Cardiology 135: 13, 2016.
11. Zhou H and Toan S: Pathological roles of mitochondrial oxidative stress and mitochondrial dynamics in cardiac microvascular ischemia/reperfusion injury. Biomolecules 10: 85, 2020.
12. Tibbo AJ and Baillie GS: Phosphodiesterase 4B: Master regulator of brain signaling. Cells 9: 1254, 2020.
13. Xie H, Zha E and Zhang Y: Identification of featured metabolism-related genes in patients with acute myocardial infarction. Dis Markers 2020: 8880004, 2020.
14. Guo H, Cheng Y, Wang C, Wu J, Zou Z, Niu B, Yu H, Wang H and Xu J: FFPM, a PDE4 inhibitor, reverses learning and memory deficits in APP/PS1 transgenic mice via cAMP/PKA/CREB signaling and anti-inflammatory effects. Neuropharmacology 116: 260-269, 2017.
15. Zhong J, Yu H, Huang C, Zhong Q, Chen Y, Xie J, Zhou Z, Xu J and Wang H: Inhibition of phosphodiesterase 4 by FCPR16 protects SH-SY5Y cells against MPP^+-induced decline of mitochondrial membrane potential and oxidative stress. Redox Biol 16: 47-58, 2018.
16. Tsai MH, Wuputra K, Lin YC, Lin CS and Yokoyama KK: Multiple functions of the histone chaperone Jun dimerization protein 2. Gene 590: 193-200, 2016.
17. Heger J, Bornbaum J, Würfel A, Hill C, Brockmann N, Gáspár R, Pálóczi J, Varga ZV, Sárközy M, Bencsik P, *et al*: JDP2 overexpression provokes cardiac dysfunction in mice. Sci Rep 8: 7647, 2018.
18. Duan Y, Cheng S, Jia L, Zhang Z and Chen L: PDRPS7 protects cardiac cells from hypoxia/reoxygenation injury through inactivation of JNKs. FEBS Open Bio 10: 593-606, 2020.
19. Livak KJ and Schmittgen TD: Analysis of relative gene expression data using real-time quantitative PCR and the 2(-Delta Delta C(T)) method. Methods 25: 402-408, 2001.
20. Rocha EAV: Fifty years of coronary artery bypass graft surgery. Braz J Cardiovasc Surg 32: 2-3, 2017.
21. Wang MX, Liu X, Li JM, Liu L, Lu W and Chen GC: Inhibition of CACNA1H can alleviate endoplasmic reticulum stress and reduce myocardial cell apoptosis caused by myocardial infarction. Eur Rev Med Pharmacol Sci 24: 12887-12895, 2020.
22. Chen YQ, Yang X, Xu W, Yan Y, Chen XM and Huang ZQ: Knockdown of lncRNA TTTY15 alleviates myocardial ischemia-reperfusion injury through the miR-374a-5p/FOXO1 axis. IUBMB Life 73: 273-285, 2021.
23. Tibaut M, Mekis D and Petrovic D: Pathophysiology of myocardial infarction and acute management strategies. Cardiovasc Hematol Agents Med Chem 14: 150-159, 2017.
24. Dong Y, Chen H, Gao J, Liu Y, Li J and Wang J: Molecular machinery and interplay of apoptosis and autophagy in coronary heart disease. J Mol Cell Cardiol 136: 27-41, 2019.
25. Shen Y, Liu X, Shi J and Wu X: Involvement of Nrf2 in myocardial ischemia and reperfusion injury. Int J Biol Macromol 125: 496-502, 2019.
26. Granger DN and Kvietys PR: Reperfusion injury and reactive oxygen species: The evolution of a concept. Redox Biol 6: 524-551, 2015.
27. Lee SJ, Lee CK, Kang S, Park I, Kim YH, Kim SK, Hong SP, Bae H, He Y, Kubota Y and Koh GY: Angiopoietin-2 exacerbates cardiac hypoxia and inflammation after myocardial infarction. J Clin Invest 128: 5018-5033, 2018.
28. Liu Z, Ma C, Gu J and Yu M: Potential biomarkers of acute myocardial infarction based on weighted gene co-expression network analysis. Biomed Eng Online 18: 9, 2019.
29. Sheng X, Fan T and Jin X: Identification of key genes involved in acute myocardial infarction by comparative transcriptome analysis. Biomed Res Int 2020: 1470867, 2020.
30. Pearse DD and Hughes ZA: PDE4B as a microglia target to reduce neuroinflammation. Glia 64: 1698-1709, 2016.
31. Zheng XY, Chen JC, Xie QM, Chen JQ and Tang HF: Anti-inflammatory effect of ciclamilast in an allergic model involving the expression of PDE4B. Mol Med Rep 19: 1728-1738, 2019.
32. Pleiman JK, Irving AA, Wang Z, Toraason E, Clipson L, Dove WF, Deming DA and Newton MA: The conserved protective cyclic AMP-phosphodiesterase function PDE4B is expressed in the adenoma and adjacent normal colonic epithelium of mammals and silenced in colorectal cancer. PLoS Genet 14: e1007611, 2018.

33. Karam S, Margaria JP, Bourcier A, Mika D, Varin A, Bedioune I, Lindner M, Bouadjel K, Dessillons M, Gaudin F, *et al*: Cardiac overexpression of PDE4B blunts β-adrenergic response and maladaptive remodeling in heart failure. Circulation 142: 161-174, 2020.
34. Xu B, Qin Y, Li D, Cai N, Wu J, Jiang L, Jie L, Zhou Z, Xu J and Wang H: Inhibition of PDE4 protects neurons against oxygen-glucose deprivation-induced endoplasmic reticulum stress through activation of the Nrf-2/HO-1 pathway. Redox Biol 28: 101342, 2020.
35. You T, Cheng Y, Zhong J, Bi B, Zeng B, Zheng W, Wang H and Xu J: Roflupram, a phosphodiesterase 4 inhibitior, suppresses inflammasome activation through autophagy in microglial cells. ACS Chem Neurosci 8: 2381-2392, 2017.
36. Ma H, Shi J, Wang C, Guo L, Gong Y, Li J, Gong Y, Yun F, Zhao H and Li E: Blockade of PDE4B limits lung vascular permeability and lung inflammation in LPS-induced acute lung injury. Biochem Biophys Res Commun 450: 1560-1567, 2014.
37. Liu XQ, Jin J, Li Z, Jiang L, Dong YH, Cai YT, Wu MF, Wang JN, Ma TT, Wen JG, *et al*: Rutaecarpine derivative Cpd-6c alleviates acute kidney injury by targeting PDE4B, a key enzyme mediating inflammation in cisplatin nephropathy. Biochem Pharmacol 180: 114132, 2020.
38. Wang S and Cao N: Uncovering potential differentially expressed miRNAs and targeted mRNAs in myocardial infarction based on integrating analysis. Mol Med Rep 22: 4383-4395, 2020.
39. Huang S, Tao W, Guo Z, Cao J and Huang X: Suppression of long noncoding RNA TTTY15 attenuates hypoxia-induced cardiomyocytes injury by targeting miR-455-5p. Gene 701: 1-8, 2019.
40. Wang XH, Liu Q and Shao ZT: Deletion of JDP2 improves neurological outcomes of traumatic brain injury (TBI) in mice: Inactivation of caspase-3. Biochem Biophys Res Commun 504: 805-811, 2018.